

Supplementary Material for

Multi-Machine Learning Ensemble Regionalization of Hydrological

Parameters for Enhancing Flood Prediction in Ungauged

Mountainous Catchments

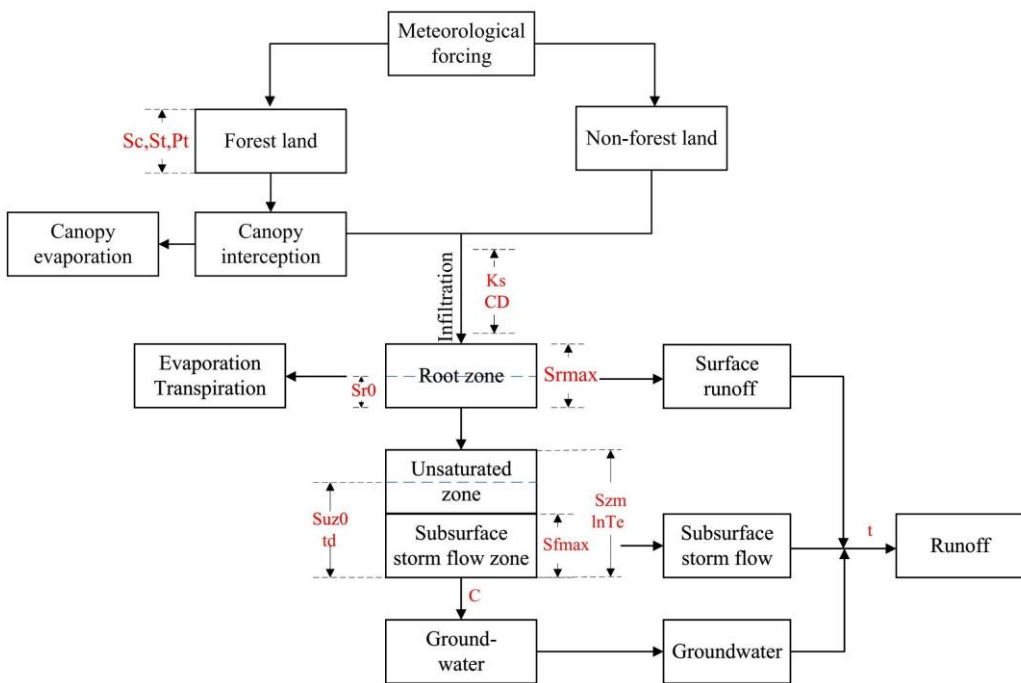
Kai Li, Linmao Guo, Genxu Wang*, Jihui Gao*, Xiangyang Sun, Peng Huang, Jinlong Li, Jiapei Ma, Xinyu Zhang

State Key Laboratory of Hydraulics and Mountain River Engineering, College of Water Resource and Hydropower, Sichuan University, Chengdu, 610000, China

*Corresponding author: Genxu Wang (wanggx@scu.edu.cn) and Jihui Gao (jgao@scu.edu.cn).

12 **The Topography-based Subsurface Storm Flow Hydrological Model (Top-SSF
13 model)**

14 The Topography-based Subsurface Storm Flow Hydrological Model (Top-SSF
15 model) is a process-based model developed to simulate the hydrological response of
16 mountainous catchments, with a particular emphasis on flash flood. The model structure
17 (Fig. S1) and its key components are detailed in the subsequent sections.



18

19 Fig.S1. Schematic diagram of the Top-SSF model structure

20 **1. Canopy Interception**

21 Canopy interception is calculated based on measured rainfall data and forest cover
22 characteristics. The process is divided into three distinct phases: canopy wetting,
23 canopy saturation, and canopy drying. In the Top-SSF model, the 1995 Gash model
24 (Gash et al., 1995) was modified and used as the canopy interception module. The
25 improved parts are as follows.

26 During the canopy humidification period, (1) the total interception equation for
27 calculating the rainfall events was converted to the hourly canopy interception equation
28 (Eq. 3), and (2) the total trunk runoff equation for calculating rainfall events was
29 converted to the hourly trunk runoff equation (Eq. 4).

30 $P'_g = -(\bar{R}/\bar{E})S_c \ln(1 - \bar{R}/\bar{E}) \quad (1)$

31 $P''_g = \bar{R}/(\bar{R} - \bar{E})(S_t/P_t) + P'_g \quad (2)$

32 $I(t) =$

33
$$\begin{cases} cP_g(t) & (P_g(t) < P'_g) \\ cP'_g + c\bar{E}(P_g(t) - P'_g)/\bar{R} + S_t & (P_g(t) \geq P''_g) \\ cP'_g + cP_t(1 - \bar{E}/\bar{R})(P_g(t) - P'_g) + c\bar{E}(P_g(t) - P'_g)/\bar{R} & (P_g(t) > P'_g, P_g(t) < P''_g) \end{cases} \quad (3)$$

34

35
$$SF(t) = \begin{cases} 0 & (P_g(t) < P'_g) \\ cP_t(1 - \bar{E}/\bar{R})(P_g(t) - P'_g) - cS_t & (P_g(t) \geq P''_g) \\ 0 & (P_g(t) > P'_g, P_g(t) < P''_g) \end{cases} \quad (4)$$

36 where: P'_g is the minimum rainfall required for the canopy to reach saturation (mm); \bar{R}
 37 is the average rainfall intensity (mm/h); \bar{E} is the average potential evaporation rate of
 38 the canopy (mm/h); S_c is the canopy storage capacity (mm); P''_g is the minimum
 39 rainfall needed in the trunk to reach saturation (mm); S_t is the trunk storage capacity
 40 (mm); P_t is the trunk runoff coefficient (%); $I(t)$ is the canopy interception
 41 (mm); $P_g(t)$ is the rainfall (mm); $SF(t)$ is the trunk runoff (mm); and c is the forest
 42 canopy closure (%), which is equal to the forest cover.

43 During the canopy saturation period, canopy interception and trunk interception
 44 are equal to zero, and canopy evaporation can be estimated as potential
 45 evapotranspiration using the Penman–Monteith equation (Rutter et al., 1971).

46 During the canopy dry period, the original Gash model assumes that when the
 47 canopy is completely dry, the drying time exceeds 8 hours (Gash et al., 1995). In the
 48 Top-SSF model, Eq. 9 was used to calculate the hourly canopy evaporation:

49 $E(t) = E_p(t)(\frac{C_h(t)}{S_c}) \quad (5)$

50 where $E(t)$ for actual canopy evaporation (mm); $C_h(t)$ is the depth of water held on
 51 canopy at time t (mm).

52 **2. Soil Infiltration**

53 In this study, infiltration is simulated using the Green-Ampt model. When surface

54 ponding occurs, the infiltration rate is determined by solving the Green-Ampt equation
55 iteratively, for which the Newton-Raphson method is employed. The infiltration rate
56 (f_{in}) is given by:

57

$$f_{in} = -\frac{Ks(CD+F_{satrt})}{Szm(1-\exp(F_{satrt}/Szm))} \quad (5)$$

58 where, f_{in} is the infiltration rate (m/h); Ks is surface hydraulic conductivity (m/h); CD
59 is capillary drive (m); F_{satrt} is the initial cumulative infiltration (m); Szm is the
60 maximum water storage capacity in the unsaturated zone (m).

61 **3. Runoff Generation and Storage Dynamics**

62 **3.1. Soil Evaporation**

63

$$E_a = E_{pt}(1 - \frac{Sr_z}{Sr_{max}}) \quad (7)$$

64 where, E_a is the Actual soil evapotranspiration (m); E_{pt} is the potential
65 evapotranspiration (m); Sr_z is the root zone water deficit (m); Sr_{max} is the maximum
66 water storage capacity of the root zone (m).

67 **3.2. Overland Flow**

68 Overland flow in the Top-SSF model consists of saturation-excess and infiltration-
69 excess components.

70 Saturation-excess flow: Occurs when groundwater table depth $S_i \geq 0$ at
71 computational cell i :

72

$$r_{s,i} = \max\{Suz_i - \max(S_i, 0), 0\} \quad (8)$$

73 where, $r_{s,i}$ is the depth of saturation excess overland flow generated at cell i (m);
74 Suz_i is the soil water storage in the unsaturated zone, at cell i (m); S_i is the
75 groundwater table depth at cell i (m).

76 Infiltration-excess flow: Activated when rainfall intensity exceeds soil infiltration
77 capacity.

78 **3.3. Subsurface storm flow**

79 Water deficit in subsurface storm flow zone ($S_{sf,i}$) is determined by topographic
80 controls:

81

$$S_{sf,i} = S_{fmax} - \frac{\left(\frac{a}{\tan \beta}\right) A_i}{\int_A \left(\frac{a}{\tan \beta}\right) dA_i} (S_{fmax} - \bar{S}_{sf}) \quad (9)$$

82 where, $S_{sf,i}$ is the water deficit in the subsurface storm flow zone at cell i (m); S_{fmax}
 83 is the maximum subsurface storm flow zone deficit (m); $\frac{a}{\tan \beta}$ is the subsurface
 84 topographic index (-); \bar{S}_{sf} is the average water deficit in the subsurface storm flow
 85 zone (m); A_i is the percentage of the catchment area occupied by cell i (%).

86 The unsaturated zone recharges the subsurface storm flow zone:

87

$$r_{v,i} = \frac{S_{uzi}}{S_i t_d} \quad (10)$$

88 where, $r_{v,i}$ is the depth of unsaturated zone recharges the subsurface storm flow zone
 89 at cell i (m); t_d is the unsaturated zone time delay per unit storage deficit (h/m).

90 The depth of storm subsurface flow generated at computational cell i , $r_{sf,i}$ is
 91 given by:

92

$$r_{sf,i} = q_{sf0} (1 - S_{sf,i} / S_{fmax}) \quad (11)$$

93 where, $r_{sf,i}$ is the depth of subsurface storm flow at cell i (m); q_{sf0} is initial
 94 subsurface storm flow (m); $S_{sf,i}$ is the water storage deficit in the subsurface storm
 95 flow zone at cell i (m).

96 The subsurface storm flow recharges the groundwater:

97

$$r_{g,i} = \min (C(S_{fmax} - S_{sf,i}), S_i) \quad (12)$$

98 where, $r_{g,i}$ is the subsurface storm flow recharge groundwater at i (m); C is the
 99 transfer coefficient (m^2/h).

100 The average water deficit of subsurface storm flow zone (\bar{S}_{sf}) and the average
 101 depth of groundwater (\bar{S}_g) in the catchment are updated as follows:

102

$$\Delta \bar{S}_{sf} / \Delta t = - \sum_{i=1}^M r_{v,i} A_i + \sum_{i=1}^M r_{sf,i} A_i + \sum_{i=1}^M r_{g,i} A_i \quad (13)$$

103

$$\Delta \bar{S}_g / \Delta t = - \sum_{i=1}^M r_{g,i} A_i + r_b \quad (14)$$

104 where, $\Delta \bar{S}_{sf}$ is the change in the average subsurface storm flow zone (m); M is the

105 total number of computational cells; $\Delta\bar{S}_g$ is the change in the average groundwater
106 level (m); Δt is the time step (h);

107 **3.4. Groundwater Flow**

108 The depth of groundwater discharge is calculate as;

109
$$r_b = e^{\ln Te - \lambda - \bar{S}_g / Szm} \quad (15)$$

110 where, r_b is depth of groundwater discharge (m); $\ln Te$ is the log of the areal average
111 of $T0$ (m^2/h); λ is the catchment average topographic index; \bar{S}_g is the catchment
112 average groundwater table depth (m).

113 **4. Flow Routing**

114 Catchment response time calculation:

115
$$T_{c,j} = t \sum_{k=1}^j \left(\frac{0.87 L_{ch,n}}{1000 S_{ch,n}} \right)^{0.385} \quad (16)$$

116 where N is the number of river subsections within the catchment; $L_{ch,n}$ is the length
117 of the river channel (km); $S_{ch,n}$ is the slope of the river segment ($m \cdot m^{-1}$); and t is the
118 time-correction coefficient (-).

119 For any simulation time step t , the proportion of the catchment area contributing
120 to the flow at the outlet is determined. If the simulation time t is greater than or equal
121 to the time of concentration for the catchment, $T_{c,N}$ (i.e., the time of concentration
122 from the most hydrologically distant point), then the entire catchment area is assumed
123 to be contributing. Otherwise, If the simulation time t is less than $T_{c,N}$, the catchment
124 is partially contributing. The proportion of the catchment area, contributing to the outlet
125 flow at time t is calculated by linear interpolation between isochrones:

126
$$AR_t = ACH_{j-1} + \frac{t - T_{c,j-1}}{T_{c,j} - T_{c,j-1}} (ACH_j - ACH_{j-1}) \quad (17)$$

127 where, AR_t is the proportion of the catchment area contributing to outlet flow at time t
128 (%); $T_{c,j}$ and $T_{c,j-1}$ are the travel times defining the boundaries of the j -th and $(j - 1)$ -th
129 isochrones, respectively (h); ACH_j and ACH_{j-1} are the cumulative proportions of
130 the total catchment area enclosed by the j -th and $(j - 1)$ -th isochrones, respectively
131 (%).

132 **References**

133 Gash, J.H.C., Lloyd, C.R.Lachaud, G. (1995). Estimating sparse forest rainfall
134 interception with an analytical model. *Journal of Hydrology*, 170(1): 79-86.
135 [https://doi.org/10.1016/0022-1694\(95\)02697-N](https://doi.org/10.1016/0022-1694(95)02697-N)

136 Rutter, A.J., Kershaw, K.A., Robins, P.C.Morton, A.J. (1971). A predictive model of
137 rainfall interception in forests, 1. Derivation of the model from observations in
138 a plantation of Corsican pine. *Agricultural Meteorology*, 9: 367-384.
139 [https://doi.org/10.1016/0002-1571\(71\)90034-3](https://doi.org/10.1016/0002-1571(71)90034-3)

140 **Hyperparameter Results**

141 **Table.S1** DT Hyperparameter Results

	max_depth	min_samples_split	min_samples_leaf
<i>lnTe</i>	53	9	3
<i>Szm</i>	922	4	2
<i>td</i>	631	4	2
<i>Sfmax</i>	253	6	2
<i>C</i>	253	2	1
<i>qsf0</i>	156	2	1
<i>t</i>	483	6	2

142

143 **Table.S2** ERT Hyperparameter Results

	n_estimators	min_samples_split	min_samples_leaf	max_features	max_depth
<i>lnTe</i>	500	2	1	0.9	15
<i>Szm</i>	200	5	1	0.5	10
<i>td</i>	500	2	1	0.9	15
<i>Sfmax</i>	500	2	1	0.2	15
<i>C</i>	500	2	1	0.9	15
<i>qsf0</i>	400	2	1	0.1	15
<i>t</i>	500	2	1	0.9	25

144

145

146

147

Table.S3 GBM Hyperparameter Results

	subsample	n_estimators	min_samples_split	min_samples_leaf	max_depth	learning_rate
<i>lnTe</i>	1.0	800	2	1	9	0.1
<i>Szm</i>	1.0	200	2	1	3	0.1
<i>td</i>	1.0	100	2	1	4	0.1
<i>Sfmax</i>	0.8	800	2	1	9	0.1
<i>C</i>	0.6	300	2	1	10	0.05
<i>qsf0</i>	0.8	800	2	1	9	0.1
<i>t</i>	0.8	800	2	1	9	0.1

148

Table.S4 KNN Hyperparameter Results

	p	n_neighbors
<i>lnTe</i>	1	20
<i>Szm</i>	3	6
<i>td</i>	1.0	4
<i>Sfmax</i>	1	7
<i>C</i>	1	4
<i>qsf0</i>	1	30
<i>t</i>	1	5

149

Table.S5 RF Hyperparameter Results

	n_estimators	max_depth	min_samples_split	min_samples_leaf
<i>lnTe</i>	1000	10	5	1
<i>Szm</i>	100	30	4	2
<i>td</i>	100	30	5	2
<i>Sfmax</i>	200	80	2	1
<i>C</i>	1000	90	10	2
<i>qsf0</i>	700	10	2	1
<i>t</i>	500	60	2	1

150

151 **Table.S6** SVM Hyperparameter Results

	tol	shrinking	kernel	gamma	C
<i>lnTe</i>	0.0001	True	rbf	10	50
<i>Szm</i>	0.0001	True	rbf	scale	0.1
<i>td</i>	0.0001	True	linear	10	1
<i>Sfmax</i>	0.0001	True	rbf	scale	0.1
<i>c</i>	0.001	True	poly	0.1	10
<i>qsf0</i>	0.0001	True	rbf	scale	0.1
<i>t</i>	0.0001	True	rbf	scale	0.1

152